

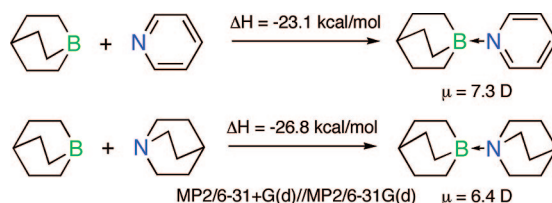
1-Pyridine- and 1-Quinuclidine-1-boraadamantane as Models for Derivatives of 1-Borabicyclo[2.2.2]octane. Experimental and Theoretical Evaluation of the B–N Fragment as a Polar Isosteric Substitution for the C–C Group in Liquid Crystal Compounds[†]

Piotr Kaszynski,^{*,‡} Serhii Pakhomov,[‡] Mikhail E. Gurskii,[§] Sergey Yu. Erdyakov,[§] Zoya A. Starikova,^{||} Konstantin A. Lyssenko,^{||} Mikhail Yu. Antipin,^{||} Victor G. Young, Jr.,[⊥] and Yurii N. Bubnov^{§,||}

Organic Materials Research Group, Department of Chemistry, Vanderbilt University, Nashville, Tennessee 37235, N. D. Zelinsky Institute of Organic Chemistry and A. N. Nesmeyanov Institute of Organoelement Compounds, Russian Academy of Sciences, Moscow, Russia 117913, and X-ray Crystallographic Laboratory, Department of Chemistry, University of Minnesota, Twin Cities, Minnesota 55455

piotr.kaszynski@vanderbilt.edu

Received November 12, 2008



The suitability of 1-borabicyclo[2.2.2]octane (**1**) as a structural element for liquid crystals was evaluated using computational methods and experimental studies of two complexes of its close analogue 1-boraadamantane (**2**). The molecular and crystal structures for 1-pyridine-1-boraadamantane [**2-P**, C₁₄H₂₀BN, *P*2₁/*m*, *a* = 8.4404(13) Å, *b* = 6.8469(10) Å, *c* = 10.5269(16) Å, β = 104.712(3)°, *Z* = 2], 1-quinuclidine-1-boraadamantane [**2-Q**, C₁₆H₂₈BN, *P*2₁/*n*, *a* = 6.6529(3) Å, *b* = 10.6665(6) Å, *c* = 19.3817(10) Å, β = 94.689(3)°, *Z* = 4], and 1-pyridine-trimethylborane [**3-P**, C₈H₁₄BN, *C*₂*m*, *a* = 6.9875(10) Å, *b* = 15.011(2) Å, *c* = 16.556(2) Å, *Z* = 8] were determined by X-ray crystallography and compared with the results of DFT and MP2 calculations. Gas-phase thermodynamic stabilities of complexes **1-P**, **1-Q**, **2-P**, and **2-Q** were estimated using a correlation between theoretical (MP2/6-31+G(d)//MP2/6-31G(d) with B3LYP/6-31G(p) thermodynamic corrections) and experimental data for complexes of BMe₃ (**3**) with amines lacking N–H bonds. The analysis showed the generally higher thermodynamic stability for the quinuclidine (**Q**) complexes compared to that of the pyridine (**P**) analogues in the gas phase and an overall order of stability of **1** > **2** > **3**. This order is paralleled by high ring strain energy of **1** (SE = 27 kcal/mol) as compared to that of 1-boraadamantane (**2**, SE = 16.5 kcal/mol). The chemical stability of **2-P** and **2-Q**, with respect to hydrolytic and oxidative reagents, is high for the pyridine derivative and satisfactory for the quinuclidine complex at ambient temperature, which implies sufficiently high stability of 1-borabicyclo[2.2.2]octane complexes for materials applications. Molecular dipole moments of 6.2 ± 0.1 and 6.0 ± 0.15 D were measured for **2-Q** and **2-P**, respectively.

Introduction

The molecular dipole moment, especially its magnitude and orientation, plays an important role in properties and applications

of liquid crystals (LC).^{1,2} Typically, the longitudinal dipole in LC, and hence the positive dielectric anisotropy Δε, is engi-

[†] Part of this work was presented in the M.Sc. Thesis of K. Bairamov, Vanderbilt University, 1997, and at XI IMEBORON, July 28–August 2, 2002, Moscow, Russia.

[‡] Vanderbilt University.

[§] N. D. Zelinsky Institute of Organic Chemistry, Russian Academy of Sciences.

^{||} A. N. Nesmeyanov Institute of Organoelement Compounds, Russian Academy of Sciences.

[⊥] University of Minnesota.

(1) Kirsch, P.; Bremer, M. *Angew. Chem., Int. Ed.* **2000**, *39*, 4216–4235.

neered by using polar terminal substituents such as $-\text{CN}^3$ and NCS^4 , among others.^{5,6} Designing mesogenic molecules with a longitudinal dipole by placing a polar group in the molecular interior is more difficult, and only some heterocycles such as pyrimidine,⁷ 1,3-dioxane,⁸ and trioxabicyclo[2.2.2]octane⁹ give rise to a molecular dipole oriented parallel to the long molecular axis.¹⁰

Several years ago, we proposed that a replacement of a C–C fragment in a liquid crystalline molecule with an isosteric polar B–N fragment can, in principle, lead to materials with a substantial $\Delta\epsilon > 0$.¹¹ If properly placed, the substitution could introduce a substantial longitudinal dipole moment without increasing the compound's absorption in the UV region. In addition, study of pairs of such isosteric compounds with different polarity would provide the first direct and molecular geometry independent measure of the influence of the dipole moment on mesogenic behavior.

In principle, the isosteric polar replacement can be applied to a C–C fragment of any hybridization; however, the stability of the resulting polar analogs containing the dative B–N bond¹² imposes practical limits. For instance, the replacement of the central $\text{C}(\text{sp}^2)\text{--}\text{C}(\text{sp}^2)$ fragment in biphenyl (Type I), an important building block for mesogenic materials,^{6,13} with the B–N leads to hydrolytically unstable 1-pyridine-1-borabenzene¹⁴ (Figure 1).¹⁵ The instability of complexes of types I and presumably II,¹⁶ which is largely related to the reactivity of the tricoordinated boron center, limits applications of borabenzene in materials.

Therefore, we focused on compounds of type III and IV (Figure 1). The sp^3 -hybridized boron center in complexes of 1-borabicyclo[2.2.2]octane (I), such as those with pyridine (I-P) and quinuclidine (I-Q), is coordinationally saturated and

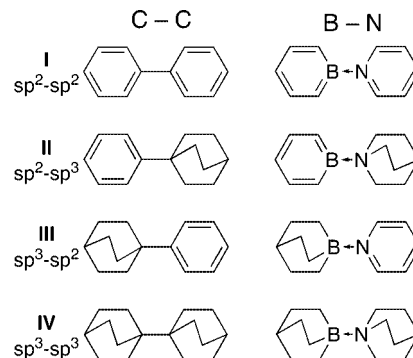


FIGURE 1. Four typical carbocyclic structural elements for calamitic liquid crystals and their polar B–N analogues.

provides substantial chemical stability to the complexes. 1-Borabicyclo[2.2.2]octane (I) is a heterocyclic analogue of bicyclo[2.2.2]octane, which is an excellent structural element for liquid crystals that exhibit highly stable nematic phases.¹⁷ Consequently, complexes I-P and I-Q are polar analogues of 1-phenylbicyclo[2.2.2]octane¹⁸ and 1,1'-bibicyclo[2.2.2]octane¹⁹ featured in a number of liquid crystalline compounds.^{6,10}

1-Borabicyclo[2.2.2]octane (I) is still an unknown ring system and inaccessible for experimental studies. To assess its potential for use as a structural element for liquid crystals, we focused on 1-boraadamantane (2), the closest known structural analogue of I.

1-Boraadamantane (2)²⁰ has been known for over three decades, and a number of its derivatives and complexes have been studied in detail.²¹ It has been postulated that the pyramidalization of the bridgehead boron atom imposed by the skeleton of 2 results in its enhanced Lewis acidity and consequently greater stability of complexes with Lewis bases. This additional stabilization energy has been estimated at about 6 kcal/mol^{22,23} by comparison of enthalpies of dissociation with the analogous complexes of BMe_3 (3). In consequence, no dissociation of the complex 2-P has been observed at 200 °C, and no decomposition upon recrystallization from alcohol,^{23,24} while the parent borane 2 reacts vigorously with air.²⁰ This relatively high thermal and chemical stability of 1-boraadamantane complexes reflects positively on the possibility to use 1-borabicyclo[2.2.2]octane (I) as a structural element of liquid crystals.¹¹

To provide a realistic assessment of 1-borabicyclo[2.2.2]octane (I) for use in molecular materials, we conducted extensive structural and chemical studies of 1-boraadamantane complexes 2-P and 2-Q. We obtained solid-state structures for 2-Q and 3-P and reproduced the original crystallographic studies for 2-P²⁵ to make all the experimental molecular structures directly comparable with each other and with theoretical results. We also measured dipole moments for 2-P and 2-Q and assessed

(2) Blinov, L. M.; Chigrinov, V. G. *Electrooptic Effects in Liquid Crystal Materials*; Springer-Verlag: New York, 1994.

(3) For example: Gray, G. W.; Harrison, K. J.; Nash, J. A. *Electron. Lett.* **1973**, *9*, 130–131; *J. Chem. Soc., Chem. Commun.* **1974**, 431–432. Eidenschink, R.; Erdmann, D.; Krause, J.; Pohl, L. *Angew. Chem., Int. Ed. Engl.* **1977**, *16*, 100.

(4) Dabrowski, R.; Dziaduszek, J.; Szczucinski, T. *Mol. Cryst. Liq. Cryst.* **1984**, *102*, 155–160; **1985**, *124*, 241–257. Dabrowski, R.; Dziaduszek, J.; Drzewinski, W.; Czuprynski, K.; Stolarz, Z. *Mol. Cryst. Liq. Cryst.* **1984**, *191*, 171–176.

(5) Toyne, K. J. In *Thermotropic Liquid Crystals*; Gray, G. W., Ed.; Wiley: New York, 1987; pp 28–63, and references therein.

(6) Demus, D. In *Handbook of Liquid Crystals*; Demus, D., Goodby, J. W., Gray, G. W., Spiess, H.-W., Vill, V., Eds.; Wiley-VCH: New York, 1998; Vol I, pp 133–187.

(7) For example: Zschke, H. *J. Prakt. Chem.* **1975**, *317*, 617–630. Kraus, G.; Zschke, H. *J. Prakt. Chem.* **1981**, *323*, 199–206.

(8) Vorbrod, H.-M.; Deresch, S.; Kresse, H.; Wiegeleben, A.; Demus, D.; Zschke, H. *J. Prakt. Chem.* **1981**, *323*, 902–913.

(9) Paschke, R.; Zschke, H.; Hauser, A.; Demus, D. *Liq. Cryst.* **1989**, *6*, 397–407.

(10) For in-depth discussion see refs 5 and 6. For tables of liquid crystalline compounds, see: Vill, V. In *Landolt-Börnstein, Group IV, Vol. 7*; Thiem, J., Ed.; Springer: New York, 1992–1995.

(11) Kaszynski, P.; Lipiak, D. In *Materials for Optical Limiting*; Crane, R., Lewis, K., Stryland, E. V., Khoshnevisan, M., Eds.; MRS: Boston, 1995; Vol. 374, pp 341–355.

(12) Haaland, A. *Angew. Chem., Int. Ed. Engl.* **1989**, *28*, 992–1007.

(13) Collings, P. J.; Hird, M. *Introduction to Liquid Crystals, Chemistry and Physics*; Taylor & Francis: Bristol, 1997.

(14) Boese, R.; Finke, N.; Henkelmann, J.; Maier, G.; Paetzold, P.; Reisenauer, H. P.; Schmid, G. *Chem. Ber* **1985**, *118*, 1644–1654. See also: Qiao, S.; Hoic, D. A.; Fu, G. C. *Organometallics* **1997**, *16*, 1501–1502.

(15) Larger polycyclic heteroaromatic compounds exhibit greater chemical stability. Among the most stable is 10a-aza-10b-borapyrene: Bosdet, M. J. D.; Piers, W. E.; Sorensen, T. S.; Parvez, M. *Angew. Chem., Int. Ed.* **2007**, *46*, 4940–4943. For a review see: Bosdet, M. J. D.; Piers, W. E. *Can. J. Chem.* **2009**, *87*, 8–29. See also: Liu, Z.; Marder, T. B. *Angew. Chem., Int. Ed.* **2008**, *47*, 242–244.

(16) Hoic, D. A.; Wolf, J. R.; Davis, W. M.; Fu, G. C. *Organometallics* **1996**, *15*, 1315–1318.

(17) Carr, N.; Gray, G. W.; Kelly, S. M. *Mol. Cryst. Liq. Cryst.* **1985**, *130*, 265–279.

(18) Carr, N.; Gray, G. W.; Kelly, S. M. *Mol. Cryst. Liq. Cryst.* **1985**, *129*, 301–313.

(19) Reiffenrath, V.; Schneider, F. Z. *Naturforsch.* **1981**, *36a*, 1006–1008.

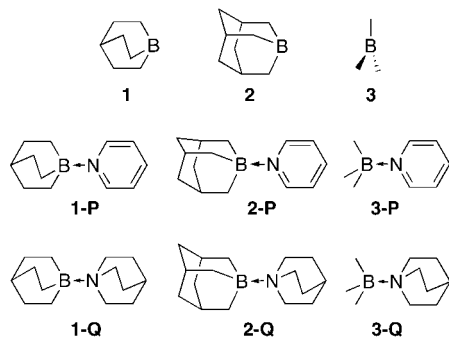
(20) Mikhailov, B. M.; Smirnov, V. N. *Bull. Acad. Sci. USSR, Div. Chem. Sci.* **1973**, 2124.

(21) Mikhailov, B. M.; Bubnov, Y. M. *Organoboron Compounds in Organic Synthesis*; Harwood Academic: New York, 1984.

(22) Mikhailov, B. M. *Pure Appl. Chem.* **1980**, *52*, 691–704.

(23) Mikhailov, B. M.; Smirnov, V. N. *Bull. Acad. Sci. USSR, Div. Chem. Sci.* **1974**, 1079–1091.

(24) Mikhailov, B. M.; Baryshnikova, T. K.; Kiselev, V. G.; Shashkov, A. S. *Bull. Acad. Sci. USSR, Div. Chem. Sci.* **1979**, 2361–2367.



their chemical stabilities. For selection of the most reliable computational method, we conducted extensive comparison of the experimental data²⁶ with theoretical thermodynamic properties for BMe₃ complexes. All of these experimental and computational results constitute the basis for the prediction of thermodynamic and dipolar properties for analogous 1-borabicyclo[2.2.2]octane complexes **1-P** and **1-Q** and two of their derivatives. Finally, strain energies for **1** and **2** were estimated to assess the prospect of a synthetic access to complexes of **1**.

Results

Selection of a Computational Method. Earlier computational studies demonstrated significant deficiencies of the HF methods and pointed out the necessity of using electron correlation for proper description of the dative bond in borane–amine complexes. Most of the studies concentrated on the parent BH₃–NH₃ system, which as a result of the small size of the molecule allows for using high level correlation methods such as QCID,²⁷ MP4(SDTQ),^{28,29} G2(MP2),³⁰ and MBPT(6)³¹ among the others.^{30,32} The standard B3LYP/6-31G(d) method was also demonstrated to be effective, giving the expected strength³³ and length of the B–N dative bond in the parent complex.³⁴ Single point MP(n) calculations at the HF geometry gave the bonding energy for BH₃–NH₃ close to the expected value, despite the calculated B–N bond being too long.^{28,32} This latter approach was shown to be successful also for methylated derivatives including Me₃B–NMe₃ (**3-NMe₃**),³² the largest borane–amine complex studied computationally to date.^{27,29,32,35–37} It appears, however, that the MP2 method overestimates the dispersion and electron correlation effects.^{28,32,34} As a result, the binding energies are larger than the experimental values, and the difference is about 4 kcal/mol for Me₃B–NMe₃ (**3-NMe₃**).³² In the latter case, almost all binding appears to be solely due to electron correlation.

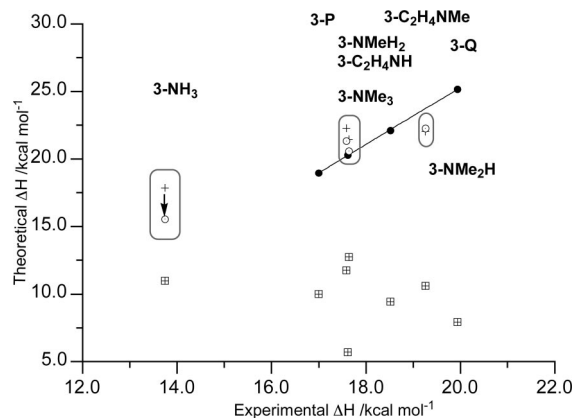


FIGURE 2. Correlation between experimental and theoretical enthalpies of dissociation for BMe₃ (**3**) complexes with amines obtained at MP2/6-31+G(d)//MP2/6-31G(d) (●, $\Delta H_{\text{theor}} = 2.12\Delta H_{\text{exp}} - 17.0$, $r^2 = 0.999$, and crosses), MP2/6-31++G(2d,p)//MP2/6-31G(d) (○) with B3LYP/6-31G(d) thermodynamic corrections, and B3LYP/6-31G(2d,p) (□) methods.

Recent computational studies demonstrated that the Minnesota functionals (M06 and M05) with extensive basis sets such as 6-311++G(3df,2p) are particularly effective in modeling the B–N dative bond.³⁷ A comparison of computed enthalpies corrected for BSSE with experimental values for the parent BH₃–NH₃ and Me₃B–NH_{3-x}Me_x derivatives demonstrated not only the correct trend but also particularly low mean absolute deviation. Such a large basis set is prohibitively expensive to use for computation of large molecular systems.

A comparison of the theoretical and experimental geometries is hindered by scarce gas-phase structural data for the B–N complexes. The use of solid-state geometries for the comparison is complicated by the apparent solid-state effect on the equilibrium geometry of BH₃–NH₃.³⁸ This, however, may be due to extensive hydrogen bonding in the solid phase of the complex³⁹ and may not significantly affect the geometry of the alkyl derivatives.

To develop a practical protocol for predicting realistic dissociation energies for complexes of **1** and **2**, we conducted a systematic comparison of theoretical enthalpies and entropies computed at several levels of theory (HF, B3LYP, and MP2) with experimental gas-phase data for six derivatives of trimethylborane (**3**).^{26,40}

Analysis of the results showed that the trend in the experimental enthalpies of formation is reproduced only with the energies obtained at the MP2 level in either single point calculations or full geometry optimization (Figure 2). In contrast, enthalpies derived from total energies obtained by methods such as HF and DFT show significant scatter of the datapoints, and all values are substantially underestimated as shown for the results of B3LYP/6-31G(2d,p) calculations in Figure 2.

Close examination of the MP2 results revealed that although the enthalpies for the complexes with amines lacking the N–H bonds computed with the 6-31G(d) bases set are overestimated, they correlate well with the experimental values, and the datapoints can be fitted to a linear function: $y = 1.56x - 6.68$,

(25) Vorontsova, L. G.; Chizhov, O. S.; Smirnov, V. N.; Mikhailov, B. M. *Bull. Acad. Sci. USSR, Div. Chem. Sci.* **1981**, 438–442.

(26) Brown, H. C. *J. Chem. Soc.* **1956**, 1248–1265, and references therein.

(27) Plumley, J. A.; Evansck, J. D. *J. Phys. Chem. A* **2007**, *111*, 13472–13483.

(28) Binkley, J. S.; Thorne, L. R. *J. Chem. Phys.* **1983**, *79*, 2932–2940.

(29) Sana, M.; Leroy, G.; Wilante, C. *Organometallics* **1992**, *11*, 781–787.

(30) Anane, H.; Boutalib, A.; Nebot-Gil, I.; Tomás, F. *J. Phys. Chem. A* **1998**, *102*, 7070–7073.

(31) Redmon, L. T.; Purvis, G. D., III; Bartlett, R. J. *J. Am. Chem. Soc.* **1979**, *101*, 2856–2862.

(32) Mo, Y.; Gao, J. *J. Phys. Chem. A* **2001**, *105*, 6530–6536.

(33) There is no independent experimental dissociation energy for BH₃–NH₃ complex, only an estimated value.

(34) Skancke, A.; Skancke, P. N. *J. Phys. Chem.* **1996**, *100*, 15079–15082.

(35) Fiacco, D. L.; Mo, Y.; Hunt, S. W.; Ott, M. E.; Roberts, A.; Leopold, K. R. *J. Phys. Chem. A* **2001**, *105*, 484–493.

(36) Schulman, J. M.; Disch, R. L. *J. Mol. Struct. (THEOCHEM)* **1995**, *338*, 109–115.

(37) Plumley, J. A.; Evansck, J. D. *J. Chem. Theory Comput.* **2008**, *4*, 1249–1253.

(38) Thorne, L. R.; Suenram, R. D.; Lovas, F. J. *J. Chem. Phys.* **1983**, *78*, 167–171.

(39) Klooster, W. T.; Koetzle, T. F.; Siegbahn, P. E. M.; Richardson, T. B.; Crabtree, R. H. *J. Am. Chem. Soc.* **1999**, *121*, 6337–6343.

(40) McLaughlin, D. E.; Tamres, M.; Searles, S., Jr.; Block, F. *J. Inorg. Nucl. Chem.* **1961**, *18*, 118–129.

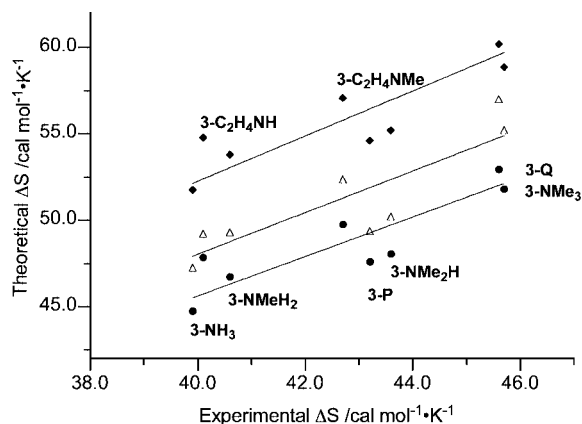


FIGURE 3. Correlation between experimental and theoretical entropies of dissociation for BMe_3 (**3**) complexes with amines obtained with HF/6-31G(d) (Δ , slope 1.20(1), $r = 0.87$), B3LYP/6-31G(d) (\bullet , slope 1.14(1), $r = 0.86$), and B3LYP/6-31G(2d,p) (\blacklozenge , slope 1.31(1), $r = 0.84$).

$r^2 = 0.997$. Addition of a diffuse function to heavy atoms in single point calculations (MP2//MP2) significantly changed the fitting function (Figure 2) and slightly improved the correlation with the experimental enthalpies. Although molecular geometry has a small effect on the MP2-calculated energies, those obtained for full geometry optimized structures correlate with the experimental values better than those from single point calculations at the DFT geometries (MP2//B3LYP).

The source of the enthalpic correction to the MP2-derived energies has little effect on the quality of the correlation with the experimental enthalpy of complexation. Thus, four sets of energies obtained at the MP2/6-31G(d) level with corrections derived from HF/6-31G(d), MP2/6-31G(d), B3LYP/6-31G(d), or B3LYP/6-31G(2d,p) calculations show the same correlation factor r of about 0.999. For the purpose of further analysis, we selected thermodynamic corrections derived from the B3LYP/6-31G(d) method.

The validity of the correlation between the experimental and theoretical enthalpies shown in Figure 2 was tested for 1-boraadamantane–pyridine complex (**2-P**). The calculated enthalpy of complex formation for **2-P** (29.9 kcal/mol) was scaled using the fitting function in Figure 2 to give 22.2 kcal/mol, which is within the experimental error of the measured value of 22.7 ± 0.7 kcal/mol.²²

Calculations for complexes derived from amines with N–H bonds were less accurate, and the error appears to depend on the number of the N–H bonds in the molecule. Thus, the largest difference between the experimental value and that expected from the partial correlation in Figure 2 was found for BMe_3 – NH_3 complex (**3-NH₃**) and the smallest for BMe_3 – NMe_2H complex (**3-NMe₂H**). The inclusion of polarization and diffuse functions in the hydrogen atom calculations significantly improved the resulting energies (boxed in areas in Figure 2). This underscores the difference between the hydrogen atom and alkyl group directly connected to the donor, and presumably the acceptor, in stabilization of the dative complexes.

Entropies of dissociation of the complexes are generally overestimated by all computational methods, and the datapoints are scattered. The slopes for the best-fit lines with experimental values range between 1.14 for the B3LYP/6-31G(d) method to 1.31 for the B3LYP/6-31G(2d,p) method (Figure 3). Entropies obtained by all three methods give a reasonable correlation with the experimental values ($r \approx 0.85$). Interestingly, despite the

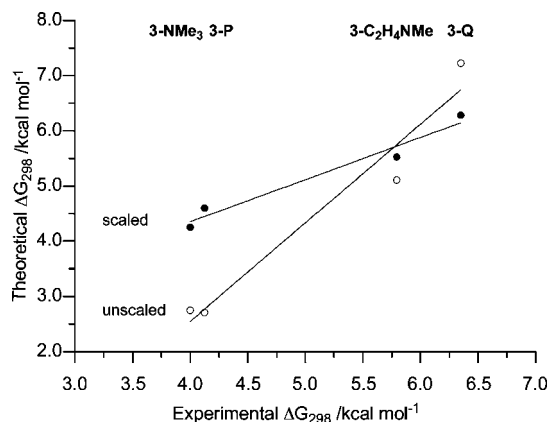


FIGURE 4. Correlation between experimental and theoretical free energy of dissociation for BMe_3 (**3**) complexes with amines at 298 K obtained with the MP2/6-31+G(d)//MP2/6-31G(d) method and B3LYP/6-31G(d) thermodynamic correction. The calculated enthalpies and entropies were unscaled (\circ , $\Delta G_{\text{theor}} = 1.8\Delta G_{\text{exp}} - 4.6$, $r^2 = 0.95$) or scaled (\bullet , $\Delta G_{\text{theor}} = 0.75\Delta G_{\text{exp}} + 1.3$, $r^2 = 0.96$) using correlations in Figures 2 and 3, respectively.

fact that both DFT methods overestimate the entropy change for the BMe_3 complex formation to different degrees (two different slopes), both calculate the ΔS of the dissociation of the 1-boraadamantane–pyridine complex (**2-P**) to be practically the same (39.4 cal/mol/K and 39.5 cal/mol/K, respectively). Consequently, the established correlations allow scaling the entropy change in the dissociation of **2-P** to 35 cal/mol/K, according to B3LYP/6-31G(d), or to 30 cal/mol/K according to B3LYP/6-31G(2d,p) results. The former seems more realistic, and the result demonstrates the difference in the treatment of flexible and rigid molecules at two different levels of theory.

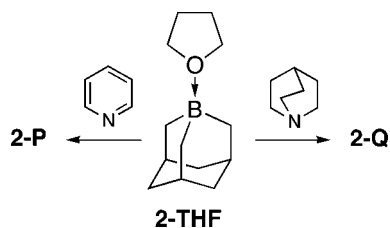
Free energies of dissociation calculated using the MP2/6-31G(d) data are expected to give linear correlation only for BMe_3 complexes with amines lacking the N–H bonds. The energies can be computed by using either DFT-derived Gibbs energy corrections or enthalpies and entropies scaled appropriately by factors defined in Figures 2 and 3. Results in Figure 4 show that the free energy of complexation calculated from scaled components gives better correlation with the experimental ΔG_{298} data ($r^2 = 0.965$) than the unscaled values ($r^2 = 0.95$, Figure 4). When forced through the origin, the slope of the former fitting line is practically a unity with a lower correlation factor ($r^2 = 0.86$).

The observed relatively poor correlation is due to the inadequate quality of the calculated entropies.

Overall, the results show that among the considered methods the most practical and reliable protocol to calculate thermodynamic properties of borane complexes involves the MP2/6-31+G(d)//MP2/6-31G(d) energies and thermodynamic corrections obtained at the B3LYP/6-31G(d) level of theory. This method represents a good compromise for complexes that do not have N–H, and possible B–H bonds, and is sufficient for assessing the thermodynamic stability of complexes of **1** and **2** with quinuclidine and pyridine. Analysis of compounds with N–H bonds require a more complete basis set for a more accurate description, but such complexes are not of our concern at the moment.

Synthesis. Complexes **2-P**⁴¹ and **2-Q** were prepared by reacting 1-boraadamantane–tetrahydrofuran complex^{24,42} (**2-THF**) with dry pyridine or quinuclidine according to a general method (Scheme 1).⁴³ This method did not permit the prepara-

SCHEME 1



tion of a double adduct of **2** with pyrazine. The complex appeared unstable under ambient conditions, and it was not pursued further.

The trimethylborane complex **3-P** was obtained according to the literature report⁴⁴ by adding excess of pyridine to BMe_3 .

Crystal and Molecular Structures. Colorless monoclinic crystals of **2-P** and **2-Q** were grown by slow sublimation at about 150 °C in an evacuated and sealed glass tube placed in a gradient sublimator. Orthorhombic crystals of **3-P** were obtained from hexane. Solid-state structures for all three compounds were determined by X-ray diffraction,⁴⁵ and their selected bond lengths and angles are shown in Tables 1 and 2.

1-Pyridine-1-boraadamantane (2-P). Low-temperature crystallographic data for **2-P** confirmed the previous room-temperature results²⁵ and found the same space group ($P2_1/m$) and similar geometrical parameters. The low-temperature experiment allowed for significant reduction of the error from approximately ± 0.005 Å in the previous studies to ± 0.002 Å in the current work. The molecules of **2-P** were found to lie on a mirror plane, which contains the pyridine ring and bisects the boraadamantane cage along the $\text{B}(1)-\text{C}(6)-\text{C}(7)\cdots\text{C}(11)$ plane (Figure 5a). The B–N bond was found to be 1.638(2) Å, which compares well to the previously reported²⁵ 1.642(6) Å for **2-P** and 1.652(7) Å for its derivative.⁴⁶ The C(6)–B bond eclipsed by the pyridine ring is markedly shorter by 0.010 Å than the other two B–C bonds, while in the pyridine the difference in the N–C distances is within the experimental error. The pyridine ring is tilted off the molecular axes defined by the C(3), N(1), and B(1) atoms by about 1°, presumably to avoid the close contact (2.297 Å) between hydrogen atoms on the pyridine and boraadamantane rings.

In the crystal structure, molecules of **2-P** form interpenetrating ideally antiparallel infinite stacks along the *b* axis in which pyridine rings are offset by 1.50 Å and separated by 3.45 Å.

1-Quinuclidine-1-boraadamantane (2-Q). Crystallographic analysis of **2-Q** revealed the quinuclidine and boraadamantane

staggered with an almost ideal overall C_3 molecular symmetry (Figure 5b). The largest deviation from the symmetry is observed in the congested region of the B–N bond. The N–C distances range from 1.498(2) to 1.507(2) Å, while the B–C bond lengths are between 1.621(3) and 1.633(3) Å. The quinuclidine ring is twisted by 19.7°. The B–N distance is 1.673(3) Å, which is longer than that in the analogous pyridine compound **2-P** by 0.035 Å and is close to 1.690(3) Å observed in a structurally similar 1-azaadamantane–1-boraadamantane complex.⁴³ The shortest nonbonding $\text{H}\cdots\text{H}$ distance between the two rings is 2.30 Å.

In the crystal structure, molecules of **2-Q** form infinite sheets in the *ab* plane with antiparallel arrangement. The separation between the closest antiparallel molecules is 6.14 Å.

1-Pyridine-trimethylborane (3-P). The molecular structure of the BMe_3 complex **3-P** is similar to that of boraadamantane **2-P** (Figure 5c). Molecules of **3-P** are found at the C_s symmetry with the pyridine ring lying in the symmetry plane. The B–N distance, 1.664(2) Å, is longer than that in **2-P** and also in most other triorganoboron complexes with pyridine.⁴⁶ The pyridine ring is tilted by 2.8°, and the closest nonbonding $\text{H}\cdots\text{H}$ distance between the methyl group and the pyridine ring is 2.29 Å.

In the crystal, molecules are arranged in interpenetrating stacks, which are rotated by 75° relative to each other. Within the columns oriented along the *a* axis, the pyridine rings are parallel to each other and separated by 3.495 Å.

Comparison with Theoretical Structures. Statistical analysis shows that all theoretical geometric parameters for **2-P**, **2-Q**, and **3-P** excluding the B–N distances compare well with the experimental values. The smallest mean difference, Δx^- , between 42 experimental and calculated bond lengths is found for the HF/6-31G(d) ($\Delta x^- = -0.002$ Å) and MP2/6-31G(d) ($\Delta x^- = -0.004$ Å) geometries. The latter Δx^- value has, however, smaller standard deviation (SD = 0.005 for MP2 vs 0.010 for the HF results), which is the smallest SD for all our computational results. For comparison, the mean difference and SD for the B3LYP/6-31G(2d,p) results are -0.008 Å and 0.006, respectively.

The critical test for the performance of the theoretical method is the reproduction of the B–N distance in the complexes. All methods overestimate the length of the dative bond, however the MP2/6-31G(d) results are closest to the experimental values with the mean difference of -0.008 Å and SD of 0.008. For comparison, the Δx^- for the B3LYP/6-31G(2d,p), B3LYP/6-31G(d) and HF/6-31G(d) results are -0.018 , -0.029 , and -0.076 Å, respectively.

The close reproduction of interatomic distances and especially the B–N bond lengths in complexes **2-P**, **2-Q**, and **3-P** by the MP2/6-31G(d) method is reflected in the small mean difference Δx^- for all bonds of -0.004 Å and small SD of 0.006 (45 parameters). These values are the smallest among all considered theoretical models, and the SD is within 3σ of the experimental uncertainty. The next best theoretical geometry was obtained with the B3LYP/6-31G(2d,p) method, which gives interatomic distances with Δx^- of -0.009 Å and SD of 0.008 Å. These statistical values are somewhat lower than those obtained with the B3LYP/6-31G(d) method (mean = -0.011 Å and SD = 0.008) or at the HF/6-31G(d) level of theory (mean = -0.007 Å and SD = 0.022).

These findings are consistent with our computational results for $\text{BMe}_3-\text{NMe}_3$. The MP2/6-31G(d) method gives a B–N distance of 1.721 Å, which is close to the experimental value

(41) Mikhailov, B. M.; Smirnov, V. N. *Bull. Acad. Sci. USSR, Div. Chem. Sci.* **1972**, 1622.

(42) Mikhailov, B. M.; Smirnov, V. N.; Kasparov, V. A. *Bull. Acad. Sci. USSR, Div. Chem. Sci.* **1976**, 2148–2153.

(43) Bubnov, Y. N.; Gurskii, M. E.; Pershin, D. G.; Lyssenko, K. A.; Antipin, M. Y. *Russ. Chem. Bull.* **1998**, 47, 1771–1777.

(44) Brown, H. C.; Schlesinger, H. I.; Cardon, S. Z. *J. Am. Chem. Soc.* **1942**, 64, 325–329.

(45) Crystal data for **2-P** (CCDC no. 709234): $\text{C}_{14}\text{H}_{20}\text{BN}$ monoclinic, $P2_1/m$, $a = 8.4404(13)$ Å, $b = 6.8469(10)$ Å, $c = 10.5269(16)$ Å, $\beta = 104.712(3)^\circ$; $V = 588.41(15)$ Å³, $Z = 2$, $T = 153(2)$ K, $\lambda = 0.71073$ Å, $R(F^2) = 0.0466$ or $R_w(F^2) = 0.1223$ (for 912 reflections with $I > 2\sigma(I)$). Crystal data for **2-Q** (CCDC no. 709232): $\text{C}_{16}\text{H}_{28}\text{BN}$, monoclinic, $P2_1/n$, $a = 6.6529(3)$ Å, $b = 10.6665(6)$ Å, $c = 19.3817(10)$ Å, $\beta = 94.689(3)^\circ$; $V = 1370.78(12)$ Å³, $Z = 4$, $T = 173(2)$ K, $\lambda = 0.71073$ Å, $R(F^2) = 0.0513$ or $R_w(F^2) = 0.1377$ (for 1814 reflections with $I > 2\sigma(I)$). Crystal data for **3-P** (CCDC no. 709233): $\text{C}_8\text{H}_{14}\text{BN}$, orthorhombic, $Cmca$, $a = 6.9875(10)$ Å, $b = 15.011(2)$ Å, $c = 16.556(2)$ Å, $V = 1736.5(4)$ Å³, $Z = 8$, $T = 153(2)$ K, $\lambda = 0.71073$ Å, $R(F^2) = 0.0646$ or $R_w(F^2) = 0.1586$ (for 876 reflections with $I > 2\sigma(I)$). For details see Supporting Information.

(46) Gurskii, M. E.; Pershin, D. G.; Potapova, T. V.; Ponomarev, V. A.; Antipin, M. Y.; Starikova, Z. A.; Bubnov, Y. N. *Russ. Chem. Bull.* **2000**, 49, 503–507.

TABLE 1. Selected Experimental and Calculated Bond Lengths and Angles for 1-Pyridine–1-borabicyclo[2.2.2]octane (**1-P**), 1-Pyridine–1-boraadamantane (**2-P**), and 1-Pyridine–BMe₃ (**3-P**)

	1-P (C ₁)		2-P (C ₅)			3-P (C ₅)		
	calcd ^{a,b}		exptl	calcd ^a		exptl	calcd ^a	
	DFT	MP2		DFT	MP2		DFT	MP2
	distances (Å)							
B(1)–N(1)	1.630	1.632	1.638(2)	1.635	1.639	1.664(2)	1.681	1.680
B(1)–C ecl	1.625	1.618	1.612(3)	1.627	1.618	1.616(3)	1.625	1.617
B(1)–C stag	1.634	1.622	1.6221(17)	1.635	1.622	1.6259(17)	1.631	1.621
N(1)–C ecl	1.344	1.349	1.344(2)	1.344	1.349	1.346(2)	1.342	1.348
N(1)–C stag	1.348	1.352	1.347(2)	1.347	1.352	1.353(2)	1.345	1.351
B(1): <i>t</i>	0.553	0.550	0.551	0.549	0.531	0.469	0.456	0.446
(Δ <i>t</i>) ^c	(+0.256)	(+0.261)		(+0.251)	(+0.240)		(+0.456)	(+0.446)
N(1): <i>t</i>	0.688	0.685	0.692	0.688	0.685	0.690	0.688	0.687
(Δ <i>t</i>) ^c	(−0.010)	(−0.021)		(−0.010)	(−0.021)		(−0.010)	(−0.019)
	angles (deg)							
C–B(1)–C (stag)	109.3	109.7	108.48(15)	109.4	110.2	113.15(15)	113.3	114.2
C–N(1)–C	118.5	119.1	118.14(16)	118.5	119.1	118.45(15)	118.4	118.8
B(1): α ^d ecl	19.9	19.9	20.0	19.7	19.2	16.9	16.3	16.0
(Δα) ^b	(+9.0)	(+9.3)		(+8.8)	(+8.5)		(+16.3)	(+16.0)
N(1): α ^d ecl	30.8	30.5	31.0	30.8	30.5	30.8	30.8	30.6
(Δα) ^b	(−0.7)	(−1.1)		(−0.7)	(−1.1)		(−0.7)	(−1.0)

^a Calculations were run at the B3LYP/6-31G(2d,p) and MP2(fc)/6-31G(d) level of theory. ^b Pseudo C₂ molecular symmetry. ^c Parameter *t* is the X–* distance and pyramidalization angle α is defined as the X–C–* angle, where * represents the midpoint between the carbon atoms adjacent to X (B or N) and the C atom is eclipsed. Δ*t* and Δα represent change in the values upon the formation of the B–N bond. ^d Angle α measured for the staggered carbon atoms is uniformly 0.1° smaller.

TABLE 2. Selected Experimental and Calculated Bond Lengths and Angles for 1-Quinuclidine–1-borabicyclo[2.2.2]octane (**1-Q**), 1-Quinuclidine–1-boraadamantane (**2-Q**), and 1-Quinuclidine–BMe₃ (**3-Q**)

	1-Q (C ₃)		2-Q (C ₃)			3-Q (C ₃)	
	calcd ^a		exptl	calcd ^a		calcd ^a	
	DFT	MP2		DFT	MP2	DFT	MP2
	distances (Å)						
B(1)–N(1)	1.697	1.662	1.673(3)	1.712	1.678	1.752	1.706
B(1)–C(1)	1.634	1.627	1.625(3) ^b	1.634	1.626	1.630	1.624
N(1)–C(1)	1.502	1.498	1.502(2) ^b	1.502	1.499	1.501	1.498
B(1): <i>t</i>	0.531	0.570	0.560	0.557	0.550	0.482	0.494
(Δ <i>t</i>) ^c	(+0.234)	(+0.281)		(+0.259)	(+0.259)	(+0.482)	(+0.494)
N(1): <i>t</i>	0.535	0.537	0.552	0.539	0.542	0.537	0.543
(Δ <i>t</i>) ^c	(+0.043)	(+0.028)		(+0.047)	(+0.033)	(+0.045)	(+0.034)
	angles (deg)						
C–B(1)–C	108.5	108.3	108.57(17) ^c	109.0	109.1	111.8	111.2
C–N(1)–C	108.0	107.9	107.32(15) ^c	107.9	107.7	107.9	107.6
B(1): α	20.5	20.4	20.4	19.9	19.8	17.2	17.7
(Δα) ^c	(+9.6)	(+9.8)		(+9.0)	(+9.1)	(+17.2)	(+17.7)
N(1): α	20.9	20.9	21.6	21.0	21.2	21.0	21.3
(Δα) ^c	(+1.4)	(+0.7)		(+1.5)	(+1.0)	(+1.5)	(+1.1)
B(1)–C–C–C	15.2	20.4	60.5(2) ^b	60.7	60.8		
(ΔΘ)	(+14.1)	(+20.4)		(+0.4)	(+0.4)		
N(1)–C–C–C	14.6	20.2	19.7(2) ^b	16.3	21.2	15.6	21.1
(ΔΘ)	(+13.2)	(+9.0)		(+14.9)	(+10.0)	(+14.2)	(+9.9)

^a DFT calculations were run at the B3LYP/6-31G(2d,p) and MP2(fc)/6-31G(d) level of theory. ^b Average value. ^c Parameter *t* is the X–* distance and pyramidalization angle α is defined as X–C–* angle where * represents the midpoint between the carbon atoms adjacent to X (B or N). Δ*t* and Δα represents change in the values upon the formation of the B–N bond.

of 1.698 ± 0.01 Å obtained in the gas phase.⁴⁷ For comparison, the same bond length was calculated as 1.732 Å at the MP2/3-21G(d) level, and the B3LYP/6-31G(2d,p) method gave 1.777 Å.

Structural Consequences of the Complex Formation. MP2-level calculations show that the boron centers in free 1-borabicyclo[2.2.2]octane (**1**) and 1-boraadamantane (**2**) are pyramidalized by about α = 10.7° (Figure 6).⁴⁸ Upon reaction with amine, the pyramidalization increases to about α = 20°, which is about

3.5° more than the same angle in the analogous complexes of trimethylborane, **3-P** and **3-Q** (Tables 1 and 2). The pyramidalization is accompanied by elongation of the B–C distances by about 0.055 Å and compression of the adjacent C–C bonds by about 0.03 Å. Upon formation of the B–N dative bond, the 1-borabicyclo[2.2.2]octane skeleton is significantly perturbed from its pseudo C_{3v} symmetry in **1** and twisted by about 17° in

(48) For comparison, the MP2/6-31G(d) level calculations for 1-adamantyl cation gave α = 8.1° and *t* = 0.204 Å, while values reported in the literature for the B3LYP/DZP++ level calculations are α = 8.4° and *t* = 0.214 Å. Yan, G.; Brinkmann, N. R.; Schaefer, H. F., III. *J. Phys. Chem. A* **2003**, *107*, 9479–9485.

(47) Kuznesof, P. M.; Kuczowski, R. L. *Inorg. Chem.* **1978**, *17*, 2308–2311.

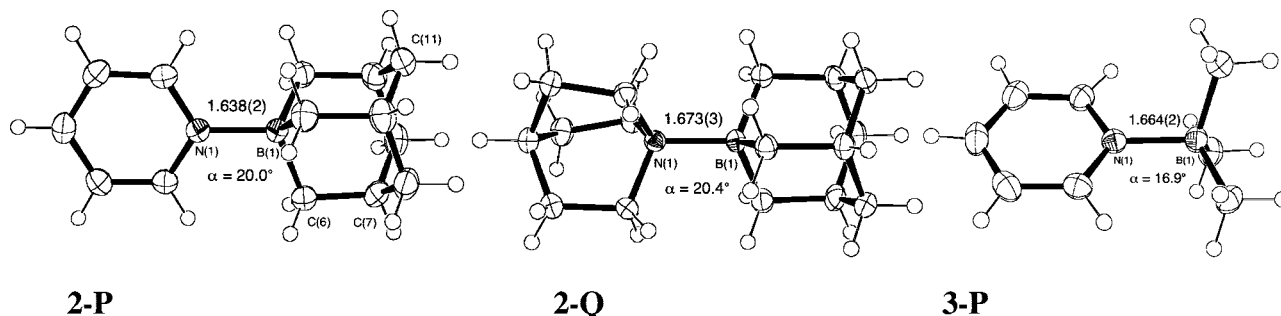


FIGURE 5. Thermal ellipsoid diagram representations of (a) 1-pyridine–1-boraadamantate (**2-P**), (b) 1-quinuclidine–1-boraadamantate (**2-Q**), and (c) 1-pyridine–trimethylborane (**3-P**) drawn at 50% probability, with the B–N bond distances and pyramidalization angles α shown. Other interatomic distances and angles are listed in Tables 1 and 2.

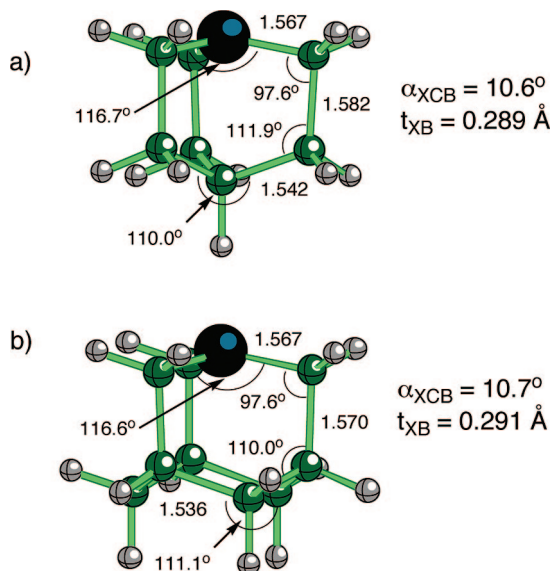


FIGURE 6. Molecular structures for (a) 1-borabicyclo[2.2.2]octane (**1**) and (b) 1-boraadamantane (**2**) optimized at the MP2/6-31G(d) level of theory at C_3 (**1**) and C_{3v} (**2**) molecular symmetry. X is the midpoint between three carbon atoms adjacent to boron.

1-P and 20.4° in **1-Q** (C_3 symmetry). In contrast, little change in dihedral angles is observed in the 1-boraadamantane skeleton due to its geometrical constraint.

The observed changes in bond lengths in the borane skeletons are not entirely due to the formation of the dative bond with amines but rather to pyramidalization of the boron center. Calculations at the MP2/6-31G(d) level show that 1-boraadamantane (**2**) and 1-borabicyclo[2.2.2]octane (**1**) pyramidalized to the level found in their quinuclidine complexes (Table 2) show elongation of the B–C distance from 1.567 to 1.630 Å, which is close to B–C bond lengths found in **1-Q** and **2-Q** (about 1.627 Å). At the same time the adjacent C–C distances are contracted by about 0.02 Å, while in the complexes the change is about 0.03 Å. Similar effects are observed in the BMe₃ complex **3-Q**.

The pyramidalization of the boron center from the level in the parent **1** and **2** to that observed in **1-Q** and **2-Q** requires energy of 14.2 and 14.8 kcal/mol, respectively, according to MP2/6-31+G(d)//MP2/6-31G(d) calculations. For comparison, pyramidalization of the parent BMe₃ (**3**) to the geometry of **3-Q** costs 20.5 kcal/mol. This difference of about 6 kcal/mol between cage boranes, **1** and **2**, and BMe₃ (**3**) provides a measure of enhanced stability of 1-boraadamantane and 1-borabicyclo[2.2.2]octane complexes.

During pyramidalization of the parent boranes, hybridization of the boron center remains practically unchanged. According to the NBO analysis of the MP2/6-31+G(d) wave function, the s character of the boron exocyclic hybrid increases insignificantly from about 0.1% to about 1% in **1** and **2**, while in BMe₃ (**3**) the LUMO changes from the pure p orbital to an orbital with about 0.4% of s character in the pyramidalized structure ($\alpha = 16.0^\circ$). A very significant change in hybridization occurs upon complexation with amines, and the exocyclic boron orbital acquires 14–18% of the s character (Table 3). The degree of s orbital contribution follows the order **3** < **2** < **1**, which is consistent with the degree of pyramidalization of the boron center in the complexes and is generally higher for the pyridine complexes with shorter B–N bonds than for quinuclidines (Tables 1 and 2).

Another consequence of pyramidalization of the boron centers is lowering of the energy of the LUMO for the boranes, which results in their increased Lewis acidity.⁴⁹ Thus, changing the angle α in BMe₃ by 17.7° lowers the energy of the LUMO by 0.36 eV. Similarly, pyramidalization in boranes **1** and **2** stabilizes the LUMO by 0.33 and 0.25 eV, respectively. Interestingly, the MP2/6-31+G(d) calculations show that the LUMO energies in **1–3** are close to each other within 0.1 eV with the lowest energy for BMe₃ and the highest for **1**. Also, the LUMO of BMe₃ remains the lowest among the three boranes after pyramidalization of the boron center.

The quinuclidine skeleton undergoes distortions during the B–N bond formation similar to those observed in borane **1**. Thus, the C–N distances expand by about 0.03 Å, and the adjacent C–C bonds contract by about 0.01 Å upon formation of the dative bond in **1-Q**, **2-Q**, and **3-Q**. The quinuclidine skeleton also twists by about 11° to reach the value of about 22° in complexes.

In contrast to quinuclidine, the geometry of the pyridine ring is little affected by the complexation with boranes. The bond lengths change by less than 0.005 Å, and the C–N–C angle expands by about 2° . This analysis based on the MP2/6-31G(d) data is consistent with crystallographic results for pyridine⁵⁰ and two of its derivatives, **2-P** and **3-P**.

Thermodynamic Stability. Thermodynamic stability of complexes of **1** and **2** with pyridine (**P**) and quinuclidine (**Q**) was assessed using the MP2/6-31+G(d)//MP2/6-31G(d) method and correlations established for derivatives **3** in Figures 2–4. Results shown in Table 4 demonstrate that in general the stability of borane complexes increase in the order **3** \ll **2** < **1**; complexes

(49) Jensen, W. B. *Chem. Rev.* **1978**, *78*, 1–22.

(50) Mootz, D.; Wussow, H.-G. *J. Chem. Phys.* **1981**, *75*, 1517–1522.

TABLE 3. Dipole Moments, Atomic Charges and Bonding for Borane–Amine Complexes^a

compound	dipole moment		natural atomic charge		bonding		
	μ_{exp}^b	μ_{calc}	q_{B}	q_{N}	B	N	WBI
1-P	na	7.3	+0.68	-0.49	sp ^{5.19} (18%)	sp ^{3.93} (82%)	0.55
2-P	6.0 ± 0.15	7.3	+0.69	-0.49	sp ^{5.38} (18%)	sp ^{3.89} (82%)	0.55
3-P	na	6.6	+0.65	-0.50	sp ^{8.10} (17%)	sp ^{3.60} (83%)	0.51
1-Q	na	6.4	+0.75	-0.58	sp ^{4.46} (15.5%)	sp ^{1.85} (85.5%)	0.50
2-Q	6.2 ± 0.1	6.4	+0.77	-0.59	sp ^{4.60} (15%)	sp ^{1.88} (85%)	0.49
3-Q	na	5.7	+0.70	-0.58	sp ^{5.30} (14.5%)	sp ^{2.03} (85.5%)	0.47

^a Natural atomic charges, hybridization indices, occupancy, and Wiberg bond indices (WBI) were obtained from the NBO analysis of the MP2/6-31+G(d)//MP2/6-31G(d) wave function. ^b Measured in benzene at 22 °C.

TABLE 4. Calculated Thermodynamic Parameters for Dissociation of Borane–Amine Complexes^a

compound	method	pyridine (P)			quinuclidine (Q)		
		ΔH	ΔS	ΔG_{298}	ΔH	ΔS	ΔG_{298}
1-borabicyclo[2.2.2]octane (1)	calcd ^b	31.8	38.3	20.3	39.6	46.1	25.8
	corr ^c	23.1	34	13.1	26.8	40	14.7
1-boraadamantane (2)	calcd ^b	29.9	39.4	18.1	36.6	44.2	23.4
	corr ^c	22.2 ^d	35	11.8	25.3	39	13.8
BMe ₃ (3)	calcd ^b	19.0	47.6	4.8	25.2	52.9	9.5
	corr ^c	17.0	42	4.6	20.0	46	6.2
	exp ^e	17.0 ± 0.2	43.2	4.1 ± 0.2	19.9 ± 1	45.6 ± 1	6.3 ± 1

^a Energies in kcal/mol and entropy in cal/mol/K. ^b MP2/6-31+G(d)//MP2/6-31G(d) electronic energy with B3LYP/6-31G(p) thermodynamic corrections. ^c Enthalpy scaled using the fitting function in Figure 2. Entropy scaled by 1.14 (Figure 3). Free energy obtained using scaled enthalpy and entropy. ^d Experimental enthalpy of formation 22.7 ± 0.7 kcal/mol.²² ^e Gas-phase experimental data for **3-P** from ref 52 and for **3-Q** from ref 51.

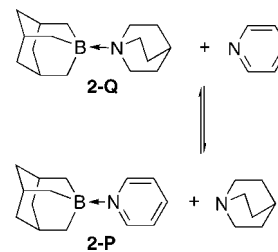
of 1-borabicyclo[2.2.2]octane (**1**) are more stable than those of 1-boraadamantane (**2**) by about 1 kcal/mol, which are more stable than those of BMe₃ (**3**) by over 5 kcal/mol. The complexes with quinuclidine appear to be more thermodynamically stable than those with pyridine by about 3 kcal/mol, which is consistent with experimental data for **3-P** and **3-Q**.^{51,52} Thus, 1-borabicyclo[2.2.2]octane–quinuclidine complex (**1-Q**) has the highest predicted enthalpy and free energy of dissociation (highest thermodynamic stability) of nearly 27 and 15 kcal/mol, respectively.

The calculated values for ΔG from appropriately scaled enthalpy and entropy represent the lower limit of the complex stability. Application of the scaling function shown in Figure 4 increases the free energy values for complexes of **1** and **2** (not **3**) by about 3 kcal/mol. While the enthalpies of formation for complexes of **1** and **2** are considered to be accurate, low quality of the calculated entropies (Figure 3) results in error of the calculated free energies of about 10–15%.

Computational results for complexes of **2** could not easily be verified experimentally. Low vapor pressure of the two 1-boraadamantane complexes preclude their studies in the gas phase using conventional methods.⁵³ Studies of the equilibrium constant for the formation of the complexes in solution are impractical because of the required very low concentrations of the complexes and high temperatures necessary to observe measurable dissociation. Both of these factors make the NMR experiment difficult and unreliable, since the amines may selectively concentrate in the gas phase above the liquid under these conditions. Therefore, we investigated solution equilibrium constants for a reaction between complex **2-Q** and pyridine (Scheme 2).

The equilibrium experiments were run for three different solutions at temperatures ranging from ambient up to 85 °C in

SCHEME 2



dioxane-*d*₈. Dioxane was chosen as the solvent on the basis of the expectation that it would not form associates with the pyridine ring as benzene does, and the complex of dioxane and 1-boraadamantane is expected to be less thermodynamically stable than those with amines (cf. **2-THF**). Equilibrium constants, *K*, were calculated using initial number of moles for pyridine and **2-Q** and the ratio of signals for pyridine in complex **2-P** and free pyridine.

Analysis of the results demonstrated a significant scattering of the datapoints. Nevertheless, the calculated equilibrium constants showed a clear trend and reproducibility in heating and cooling cycles especially above 35 °C. The data was not, however, of high enough quality to calculate accurate thermodynamic parameters for the process, but it clearly indicated that quinuclidine complex **2-Q** is more thermodynamically stable than the corresponding **2-P** complex. The obtained equilibrium constant values, *K*, fall in the range of 0.014–0.024, which corresponds to a range of free energy change of +2.3 kcal/mol to +2.6 kcal/mol for the process. This is consistent with the estimated difference of 2 kcal/mol in ΔG_{298} of complexation for **2-P** and **2-Q** (Table 4) or $\Delta\Delta G_{298}$ of 2.6 kcal/mol obtained as the difference of scaled ΔG_{298} values (see Figure 4).



Chemical Stability. Reactivity of complexes **2-P** and **2-Q** toward several solvents and reagents at two temperatures in benzene was monitored using ¹¹B NMR spectroscopy. In general, the pyridine complex **2-P** was more resistant to

(51) Brown, H. C.; Sujishi, S. *J. Am. Chem. Soc.* **1948**, *70*, 2878–2881.

(52) Brown, H. C.; Barbaras, G. K. *J. Am. Chem. Soc.* **1947**, *69*, 1137–1144.

(53) Brown, H. C.; Taylor, M. D.; Gerstein, M. *J. Am. Chem. Soc.* **1944**, *66*, 431–435.

TABLE 5. Homodesmotic Strain Energy for Boranes **1** and **2**, Their Complexes with Pyridine, and the Corresponding Hydrocarbons

	Compound	Strain Energy ^a [kcal/mol]	
		ΔE_0	ΔH
X = B	1-Borabicyclo[2.2.2]octane (1)	26.8	27.1
X = CH	Bicyclo[2.2.2]octane	9.8	10.6 ^b
X = B-Pyr	1-Borabicyclo[2.2.2]octane-1-Pyridine (1-P)	13.3	14.3
X = C-Ph	1-Phenylbicyclo[2.2.2]octane	6.3	7.5
			
X = B	1-Boraadamantane (2)	16.3	16.6
X = CH	Adamantane	2.3	3.2 ^c
X = B-Pyr	1-Boraadamantane-1-Pyridine (2-P)	4.7	5.7
X = C-Ph	1-Phenyladamantane	-1.4	-0.2

^a Calculated using MP2/6-31+G(d)//MP2/6-31G(d) energies and B3LYP/6-31G(d) thermodynamic corrections. ^b Calculated from experimental standard heats of formation:⁵⁷ 10.4 kcal/mol; lit.⁵⁸ SE 11.0 kcal/mol. ^c Calculated from experimental standard heats of formation:⁵⁷ 5.1 kcal/mol; lit.⁵⁸ SE 6.5 kcal/mol.

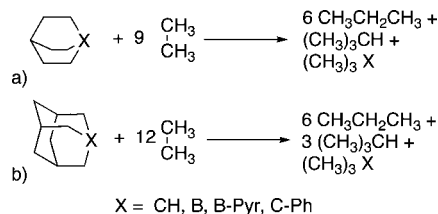
decomposition than the quinuclidine analogue. In both cases the ¹¹B NMR signal for the decomposition product was shifted downfield by >20 ppm from that of the starting complex. This is consistent with the presence of a B–O bond, but no attempt was made to identify these products. No reaction was observed for **2-P** at ambient temperature in the presence of 10% v/v of methanol, acetic acid, or *tert*-butyl peroxide after 48 h. Trifluoroacetic acid reacted with **2-P** to give about 7% and 19% of decomposition products in 6 and 23 h, respectively. After 15 min at 50 °C, 18%, 32%, and 81% of **2-P** was transformed to products in benzene solutions containing methanol, acetic, and trifluoroacetic acids, respectively.

The quinuclidine complex **2-Q** was found to be significantly less stable. A reaction of **2-Q** with CF₃COOH was quantitative after 10 min at ambient temperature. In solutions containing methanol and *tert*-butyl peroxide, **2-Q** gave 35% and 28% of conversion respectively after 1 h, or 77% after 18 h with *tert*-butyl peroxide. The rate of decomposition was significantly accelerated at 50 °C. Thus, **2-Q** reacted with methanol and acetic acid to the extent of 35% and completely decomposed with *tert*-butyl peroxide after only 15 min.

Dipole Moment. Dipole moment measurements for complexes **2-P** and **2-Q** in benzene solutions gave values of 6.0 ± 0.15 and 6.2 ± 0.1 D, respectively (Table 3). This is consistent with values reported for other borane–amine complexes.⁵⁴ The experimental value obtained for the quinuclidine complex **2-Q** is in good agreement with results of DFT and MP2 calculations, whereas that for the pyridine analogue is significantly lower. This can be attributed to the solvent effect⁵⁵ and relatively strong π – π interactions of benzene and formal pyridinium ring, whereas the aliphatic quinuclidine presumably less affected by the solvent.

Ring Strain. Homodesmotic strain energies⁵⁶ (SE) for boranes **1** and **2**, pyridine derivatives **1-P** and **2-P**, and their hydrocarbon analogues were estimated according to Scheme 3 using the MP2/6-31+G(d)//MP2/6-31G(d) energies (Table 5).

SCHEME 3



In general, compounds containing the bicyclo[2.2.2]octane skeleton are more strained than the analogous adamantane derivatives. 1-Borabicyclo[2.2.2]octane (**1**) has the highest SE of about 27 kcal/mol, which is higher by 10.5 kcal/mol than the SE for 1-boraadamantane (**2**). Both boranes **1** and **2** are significantly more strained than their hydrocarbon analogs by 16.5 kcal/mol for the former and 13.4 kcal/mol for the adamantane pair. Upon complexation with pyridine, the SE of borane skeleton **1** is reduced by about 13 kcal/mol to about 14 kcal/mol in **1-P**, and the SE of 1-boraadamantane skeleton by about 11 kcal/mol. In comparison, SE for bicyclo[2.2.2]octane and adamantane is lowered by only about 3 kcal/mol upon phenylation. This excess energy present in the parent boranes is related to the sterically imposed pyramidalization of the boron center, which adopts the favorable tetrahedral geometry upon coordination with a Lewis base.

Discussion

The availability of the gas-phase thermodynamic data for BMe₃ complexes and molecular structures for **2-P**, **2-Q**, and **3-P** permitted the testing of several computational methods and consequently the development of a practical computational protocol for treatment of this class of compounds. In agreement with previous findings, our results demonstrated the necessity of correlation methods for correct description of the dative bond

strength and the geometry of borane complexes. We found that the MP2/6-31G(d) and MP2/6-31+G(d)//MP2/6-31G(d) methods with DFT-derived thermodynamic corrections perform well for complexes of boranes, although the computed energies are overestimated and require scaling. For borane–amine complexes that do not contain N–H bonds, a high quality linear correlation was found that relates the computed and gas-phase experimental enthalpies of dissociation and can be used for prediction of realistic enthalpies for complexes of 1-boraadamantane (**2**) and 1-borabicyclo[2.2.2]octane (**1**) with pyridine and quinuclidine. Whereas enthalpies of complexation are well correlated with the experimental values, the entropy change is rather poorly reproduced by the DFT method with standard basis sets. This gives rise to a substantial uncertainty (about 10–15%) of ΔG for the dissociation process.

The MP2/6-31G(d) method also well reproduces interatomic distances in the borane complexes. The calculated bond lengths, and particularly the B–N distance, in **2-P**, **2-Q**, and **3-P** are within 3σ of the experimental values, which is a substantially better result than those of HF or DFT calculations. This suggests that the geometries calculated at the MP2/6-31G(d) level of theory for 1-borabicyclo[2.2.2]octane (**1**) and its derivatives are realistic.

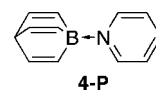
Overall the developed computational protocol offers a good compromise between accuracy and efficiency especially for large systems such as those containing **1** and **2** and provides a realistic estimate of the B–N bond strength. The protocol includes calculations of total energies at the MP2/6-31+G(d)//MP2/6-31G(d) level and thermodynamic corrections obtained with the B3LYP/6-31G(d) method. The resulting enthalpies are scaled according to $\Delta H_{(\text{exp})} = (\Delta H_{(\text{calcd})} + 17.0)/2.12$, and the entropies are scaled by 1.14. The free energies ΔG are obtained from the scaled enthalpies and entropies, and are believed to represent the lower limit of stability for complexes of **1** and **2**.

Calculations show that the stability of the borane complexes increases in the order **3** < **2** < **1** and approximately correlates with the B–N distances: the shorter the distance, the more stable the complex. This is in agreement with general trends in properties of dative bonds.¹² The estimated enthalpies of formation for complexes of 1-borabicyclo[2.2.2]octane, **1-P** and **1-Q**, are about 1 kcal/mol higher than those calculated for 1-boraadamantane analogues and over 6 kcal/mol more than those for complexes of BMe₃. This represents a significant increase in stability of the dative bond relative to **3**, and it originates in the pyramidalization of the boron centers in the parent boranes **1** and **2**. The thermodynamic stability of complexes of **1** and **2** relative to those of **3** is even higher as a result of smaller entropy change in the dissociation of the former complexes that contain the rigid 1-boraadamantane (**2**) and 1-borabicyclo[2.2.2]octane (**1**) skeletons. Thus, the entropy change in the formation of **1-P** and **2-P** is estimated at about –35 cal/mol/K, which is less than –42 cal/mol/K estimated or –43 cal/mol/K measured⁵² for **3-P**. This difference results in additional stability of complexes of **1** and **2** relative to those of **3** by about 2 kcal/mol at 25 °C.

The behavior of borane complexes in the condensed phase appears to be different from that in the gas phase. The experimental equilibrium data for **2-P** and **2-Q** shows that the difference in the enthalpy of dissociation decreases from the estimated 3.1 kcal/mol in the gas phase to <1 kcal/mol found experimentally. IPCM calculations for **3-P** and **3-Q** in a dielectric medium indicate that the enthalpy of formation of

the former is little changed (<0.1 kcal/mol), whereas the quinuclidine complex **3-Q** is destabilized by nearly 0.3 kcal/mol relative to the gas phase. Considering the simplicity of the IPCM solvation model and the lower enthalpy of complexation in PhNO₂ solutions by 1.7 kcal/mol measured for **3-P**,⁵⁹ the dielectric medium effect on the complex stability may be significantly underestimated. Consequently, the actual destabilization of **3-Q** in solutions may be much greater and the actual difference in the ΔH for **3-P** and **3-Q** may be larger. Unfortunately, experimental data for the stability of both BMe₃ complexes in solution is not known. However, these results are consistent with the observed lower chemical stability of **2-Q** compared to that of **2-P** in solutions, which involves the complex dissociation and generation of free borane.

The developed computational protocol can be used to assess the gas-phase stability of other complexes of **1** such as those with substituted pyridine and double complexes with pyrazine or DABCO and also the properties of complexes of 1-borabarrelene (**4**), a triply unsaturated analogue of **1**, such as **4-P**.



Recently, several substituted derivatives of the parent 1-pyridine-1-borabarrelene (**4-P**) were investigated by crystallographic and thermal analysis methods.⁶⁰ Experiments demonstrated a short B–N distance in two of the derivatives (about 1.585 Å), which indicates significantly tighter binding in **4-P** than in **2-P** or **1-P**. This tight binding is paralleled by unusually high thermal stability of derivatives of **4-P**, which apparently do not undergo pyridine ligand exchange even at 200 °C.⁶⁰ Our MP2 level calculations estimate the enthalpy of dissociation for the parent **4-P** at 33.6 kcal/mol, which is higher by about 10 kcal/mol than that for **1-P** (Table 4). The calculated free energy of dissociation of **4-P** is 24.3 kcal/mol (lower limit), which is larger than expected by about 1 kcal/mol in part due to higher rigidity of the 1-borabarrelene ring and consequently smaller entropy of dissociation (31 cal/molK) than for **1-P** (34 cal/molK). Calculations indicate that the high binding enthalpy observed in **4-P** is largely due to pronounced pyramidalization of the boron center in the parent **4** ($\alpha = 15^\circ$ and $t = 0.41$ Å) imposed by the sp²-hybridized skeletal carbon atoms. The calculated B–N distance is 1.601 Å, and the dipole moment is 8.0 D. Overall, the stability of **1-P** is expected to be somewhat higher than that of 1-boraadamantane complexes but significantly less than that of 1-borabarrelene complexes.

Calculations demonstrate that introduction of an alkyl or alkoxy substituent in the 4 position of pyridine modestly increases thermodynamic stability of the complex (Table 6). For instance, the enthalpy of complexation for **1-PEt** is higher by 0.3 kcal/mol than that for the parent **1-P**. This increase of enthalpy is lower than that measured for **3-PMe** relative to **3-P**, although the former has large uncertainty.⁵² A slightly larger stabilization, by about 0.6 kcal/mol, is calculated for 4-methoxy pyridine complex **1-POMe** (Table 6). A pentyl derivative of this complex is an isosteric polar analogue of a weakly polar nematic liquid crystal **5**,¹⁸ and therefore is expected to exhibit

(54) Nöth, H.; Beyer, H. *Chem. Ber.* **1960**, *93*, 939–944. Bax, C. M.; Katritzky, A. R.; Sutton, L. E. *J. Chem. Soc.* **1958**, 1258–1262.

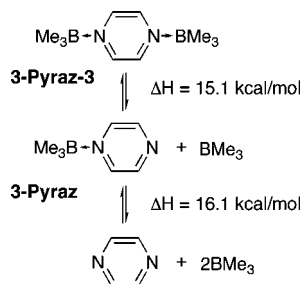
(55) Prezhdo, V. V.; Degtereva, L. I.; Lutskii, A. E. *Russ. J. Gen. Chem.* **1981**, *51*, 772–777.

(56) George, P.; Trachtman, M.; Bock, C. W.; Brett, A. M. *Tetrahedron* **1976**, *32*, 317–323.

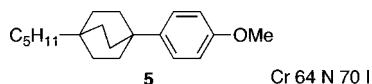
TABLE 6. Predicted Thermodynamic Parameters for Selected Complexes of **1**^a

R		ΔH	ΔS	ΔG_{298}
H	1-P	23.1	33.6	13.1
Et	1-PEt	23.4	34.2	13.2
MeO	1-POMe	23.7	^b	

^a Energies (kcal/mol) and entropy (cal/mol/K) were obtained using MP2/6-31+G(d)//MP2/6-31G(d) electronic energies and B3LYP/6-31G(p) thermodynamic corrections and scaled as shown in Figures 2 and 3. Free energy was obtained using scaled ΔH and ΔS . ^b Not obtained; see ref 61.

SCHEME 4

mesogenic properties. Unfortunately, the modest enthalpic gain in these complexes is nearly entirely compensated by increase in entropy, which is also observed⁵² for **3-PMe** relative to **3-P**.



Formation of double complexes of boranes such as those with pyrazine and DABCO are less favorable than the mono complexes. Calculations demonstrated that the formation of the monoadduct of BMe_3 with pyrazine, **3-Pyraz**, is less exothermic by 0.9 kcal/mol than that with pyridine (**3-P**). The addition of the second molecule of BMe_3 to form the bis adduct **3-Pyraz-3** is still less favorable by another 1 kcal/mol (Scheme 4) due to the electron-withdrawing effect of the second nitrogen atom that is already coordinated to BMe_3 . Consequently, bis complexes of 1-boraadamantane and 1-borabicyclo[2.2.2]octane are expected to be less stable than those with pyridine (**2-P** and **1-P**) by about 2 kcal/mol. This estimate is consistent with the experimental observation that the bis adduct of 1-boraadamantane to pyrazine (**2-Pyraz-2**) was unstable during attempted purification.

The dipole moments of the complexes increase with decreasing length of the dative bond, which is related to a more extensive charge transfer at shorter bond distances.³⁵ Thus, dipole moments calculated for complexes of **1** and **2** are generally higher than for the analogous derivatives of BMe_3

(**3**) and complexes of pyridine are more polar by about 1 D than the analogous derivatives of quinuclidine (Table 3). This is consistent with larger atomic charges and higher bond indices (WBI in Table 3). The dipole moment of **1-P** is calculated to be over 7 D and even higher in the 4-alkyl and alkoxy derivatives. Such a high dipole moment is desired for electro-optical applications.

Finally, a comment on the prospect of synthesis of the 1-borabicyclo[2.2.2]octane skeleton. 1-Boraadamantane (**2**) has a moderate strain energy (SE) of about 16 kcal/mol (Table 5), which does not interfere with its efficient (>70% yield) formation.²⁰ Calculations show that the SE of the parent **2** is reduced by over 10 kcal/mol upon complexation with a Lewis base, and **2** is also readily prepared directly as THF (**2-THF**)^{24,42} or pyridine (**2-P**)⁴¹ complexes. Similar reduction of strain energy is observed for the parent borane **1** when complexed with pyridine. The complex is less strained than the parent **2** by about 2 kcal/mol and more strained than **2-P** (by 8.6 kcal/mol), the carbocyclic analogue (by 6.8 kcal/mol), and the parent bicyclo[2.2.2]octane (by 3.7 kcal/mol). Since 1-boraadamantane and its complexes and also derivatives of bicyclo[2.2.2]octane are routinely prepared in good yields, complexes of **1** should also be accessible by cyclization of appropriate borane precursors in the presence of a Lewis base.

Conclusions

Extensive comparison and analysis of experimental and theoretical data for BMe_3 complexes allow the development of a practical protocol for estimation of thermodynamic stabilities of borane complexes that do not possess N–H bonds. The protocol was used to predict thermodynamic stabilities of complexes of 1-borabicyclo[2.2.2]octane (**1**) and 1-boraadamantane (**2**) with quinuclidine, pyridine, and two of its derivatives. Calculations and experimental results for **2-P** lead to the expectation of substantial chemical stability for complexes of **1** with 4-substituted pyridines at ambient temperatures. Such a level of chemical stability may be sufficient for fundamental studies of structure–property relationships in liquid crystals and possible applications, which warrants experimental investigation of this intriguing ring system. Further stabilization of the borane–amine complexes can be accomplished by introduction of unsaturation to the skeleton of **1** and consequent additional pyramidalization of the boron center observed in 1-borabarrelene (**4**).

Overall, 1-borabicyclo[2.2.2]octane represents an attractive and realistic synthetic goal with interesting implications for materials chemistry.

Computational Methods

Quantum-mechanical calculations were carried out using the Linda-Gaussian 98 package⁶² on a Beowulf cluster of 16 processors. Geometry optimizations were undertaken at the HF, B3LYP,^{63,64} and MP2(fc)⁶⁵ levels of theory using appropriate symmetry constraints, tight convergence limits, and the GDHS algorithm. All methods used the standard 6-31G(d) basis sets, and the DFT calculations used 6-31G(2d,p) basis sets augmented with diffuse function for non-hydrogen atoms. Vibrational frequencies were used to characterize the nature of the stationary points and to obtain thermodynamic parameters. Zero-point energy (ZPE) corrections were scaled by 0.915 (HF), 0.9804 (DFT), and 0.9670 (MP2).⁶⁶ No correction for the basis set superimposition errors was used. The Wiberg bond order indices, atomic charges, and hybridization

(61) Repeated geometry optimizations of unconstrained **1-POMe** at the B3LYP/6-31G(d) level of theory always gave a small imaginary frequency of -7.5 cm^{-1} , which is related to the torsional motion of the bicyclo[2.2.2]octane ring. The imaginary frequency was absent at the B3LYP/6-31G(2d,p) level of theory.

(57) NIST Chemistry WebBook (<http://webbook.nist.gov/chemistry/>) and references therein.

(58) Schleyer, P. v. R.; Williams, J. E.; Blanchard, K. R. *J. Am. Chem. Soc.* **1970**, *92*, 2377–2386.

(59) Brown, H. C.; Gintis, D. *J. Am. Chem. Soc.* **1956**, *78*, 5378–5383.

(60) Wood, T. K.; Piers, W. E.; Keay, B. A.; Parvez, M. *Org. Lett.* **2006**, *8*, 2875–2878.

parameters were obtained using the NBO⁶⁷ algorithm supplied in the Gaussian 98 package.

Following general recommendations,⁶⁸ energy changes and differences were derived as the differences of MP2 energies of individual species computed using the diffuse function-augmented 6-31+G(d) basis set at the geometries obtained with the 6-31G(d) basis set (single point calculations). Thermodynamic corrections were obtained using either the 6-31G(d) or 6-31G(2d,p) basis set.

Experimental Section

1-Pyridine-1-boraadamantane (2-P).⁴¹ Mp 150 °C (sealed tube) (lit.⁴² 160–162 °C); ¹H NMR (400 MHz, CDCl₃) δ 0.77 (s, 6H), 1.62 (d, *J* = 11.5 Hz, 3H), 1.71 (d, *J* = 11.6 Hz, 3H), 2.21 (s, 6H), 7.52 (t, *J* = 6.4 Hz, 2H), 7.89 (td, *J*₁ = 7.6 Hz, *J*₂ = 1.4 Hz, 1H), 8.59 (d, *J* = 5.9 Hz, 2H); ¹³C NMR (100 MHz, CDCl₃) δ 32.9, 33.4 (br), 40.14, 125.0, 138.5, 144.6; ¹¹B NMR (128 MHz, CDCl₃) δ -4.5 (s); UV, λ_{max} (log ε) 250 nm (3.30); EIMS, *m/z* 472–477 (max at 475, 11), 457–462 (max at 460, 14), 442–450 (max at 446, 20). Anal. Calcd for C₁₄H₂₀BN: C, 78.90; H, 9.46; N, 6.57. Found: C, 78.84; H, 9.50; N, 6.54.

1-Quinuclidine-1-boraadamantane (2-Q). Mp > 250 °C (sealed tube); ¹H NMR (400 MHz, CDCl₃) δ 0.49 (d, *J* = 3.2 Hz, 6H), 1.47 (d, *J* = 11.5 Hz, 3H), 1.57 (d, *J* = 11.7 Hz, 3H), 1.63–1.70 (m, 6H), 1.93 (sept, *J* = 3.2 Hz, 1H), 2.14 (s, 3H), 2.85 (t, *J* = 7.8 Hz, 6H); ¹³C NMR (100 MHz, CDCl₃) δ 20.3, 24.7, 27.2 (br), 32.8, 40.4, 46.2; ¹¹B NMR (128 MHz, CDCl₃) δ -4.4 (s). Anal. Calcd for C₁₆H₂₈BN: C, 78.37; H, 11.51; N, 5.71. Found: C, 78.17; H, 11.71; N, 5.70.

1-Pyridine-trimethylborane (3-P). This compound was prepared by adding an excess of pyridine to trimethylborane⁶⁹ according to a literature procedure.⁴⁴ ¹H NMR (200 MHz, CDCl₃) δ -0.05 (s, 9H), 7.49 (t, 2H), 7.85 (t, 1H), 8.15 (d, 2H); ¹³C NMR (50 MHz, CDCl₃) δ 2.50 (br), 124.6, 137.9, 146.3; ¹¹B NMR (64 MHz, CDCl₃) δ -0.24.

(62) Gaussian 98, Revision A.9; Frisch, M. J.; Trucks, G. W.; Schlegel, H. B.; Scuseria, G. E.; Robb, M. A.; Cheeseman, J. R.; Zakrzewski, V. G.; Montgomery, J. A.; Stratmann, R. E., Jr.; Burant, J. C.; Dapprich, S.; Millam, J. M.; Daniels, A. D.; Kudin, K. N.; Strain, M. C.; Farkas, O.; Tomasi, J.; Barone, V.; Cossi, M.; Cammi, R.; Mennucci, B.; Pomelli, C.; Adamo, C.; Clifford, S.; Ochterski, J.; Petersson, G. A.; Ayala, P. Y.; Cui, Q.; Morokuma, K.; Malick, D. K.; Rabuck, A. D.; Raghavachari, K.; Foresman, J. B.; Cioslowski, J.; Ortiz, J. V.; Baboul, B. B.; Stefanov, A. G.; Liu, G.; Liashenko, A.; Piskorz, P.; Komaromi, I.; Gomperts, R.; Martin, R. L.; Fox, D. J.; Keith, T.; Al-Laham, M. A.; Peng, C. Y.; Nanayakkara, A.; Challacombe, M.; Gill, P. M. W.; Johnson, B.; Chen, W.; Wong, M. W.; Andres, J. L.; Gonzalez, C.; Head-Gordon, M.; Replogle, E. S.; Pople, J. A. Gaussian, Inc.: Pittsburgh, PA, 1998.

(63) Becke, A. D. *J. Chem. Phys.* **1993**, *98*, 5648–5652.

(64) Lee, C.; Yang, W.; Parr, R. G. *Phys. Rev. B* **1988**, *37*, 785–789.

(65) Möller, C.; Plesset, M. S. *Phys. Rev.* **1934**, *46*, 618. Head-Gordon, M.; Pople, J. A.; Frisch, M. J. *Chem. Phys. Lett.* **1988**, *153*, 503.

(66) Scott, A. P.; Radom, L. *J. Phys. Chem.* **1996**, *100*, 16502–16513.

(67) Glendenning, E. D.; Reed, A. E.; Carpenter, J. E.; Weinhold, F. NBO version 3.1.

(68) Clark, T.; Chandrasekhar, J.; Spitznagel, G. W.; Schleyer, P. v. R. *J. Comput. Chem.* **1983**, *4*, 294–301.

(69) Wiberg, E.; Ruschmann, W. *Chem. Ber.* **1937**, *70*, 1583–1591.

Dissociation Constant Measurements. Two solutions of 1-quinuclidine-1-boraadamantane (**2-Q**) and pyridine in dry dioxane-*d*₈ in amounts of ~5 × 10⁻⁵ and ~5 × 10⁻⁶ mol, respectively, were prepared by weighting the solvent and solutes with accuracy of >99%. Pyridine was added as a stock solution in dioxane-*d*₈. The ratio of free pyridine to 1-pyridine-1-boraadamantane (**2-P**) was obtained from integration of ¹H NMR signals at 7.26 ppm (m, 2H^β) and at 7.51 ppm (tm, 2H^β) ascribed to free pyridine (**P**) and complex **2-P**, respectively. The data was collected on heating and subsequently cooling every 10 K in the range of temperatures 318–358 K. The solutions were allowed to equilibrate for about 15 min before each measurement. The equilibrium constants obtained upon heating and cooling in two experiments were averaged and used in subsequent calculations. Temperature calibration was done by using the separation of two NMR signals in the ethylene glycol standard. The equilibrium constant *K* was obtained from the formula:

$$K = \frac{x^2(n_p)}{x(n_{2Q} - n_p) + n_{2Q}} \quad (1)$$

in which *x* is the ratio of **2-P** to **P** established by NMR, *n*_{2Q} is the initial number of moles of **2-Q**, and *n*_p is the initial number of moles of pyridine.

Dipole Moment Measurements. Dipole moments for complexes **2-P** and **2-Q** were obtained from dielectric and refractive measurements conducted for a set of 4–5 low concentration solutions in benzene at 25 °C according to a general protocol.⁷⁰ The measurements were repeated for several series of solutions and the resulting dipole moment values were averaged.

Chemical Stability Measurements. Stability of complexes **2-P** and **2-Q** was assessed at 25 and 50 °C in dry benzene-*d*₆ containing 10% v/v of an appropriate reagent (methanol, acetic acid, or trifluoroacetic acid) or three times molar excess of *tert*-butyl peroxide. The stability was estimated from integration of ¹¹B NMR signals belonging to the starting 1-boraadamantane complex (about -0.2 ppm) and products of decomposition appearing at about 20, 37, and 57 ppm. The ¹¹B NMR spectra were taken periodically over a period of time up to 2 days. The tabulated results are shown in Supporting Information.

Acknowledgment. Financial support for this work was received from the National Science Foundation (DMR-9703002, DMR-00111657, DMR-0606317).

Supporting Information Available: General procedures, chemical stability data, crystallographic data in CIF format, listings of fractional coordinates, atom positions for **2-P**, **2-Q**, and **3-P**, and archive of computational results for the parent boranes **1–4** and their complexes. This material is available free of charge via the Internet at <http://pubs.acs.org>.

JO802504C

(70) Cumper, C. W. N.; Vogel, A. I.; Walker, S. *J. Chem. Soc.* **1956**, 3621–3628.